Early postnatal behavioral, cellular, and molecular changes in models of Huntington disease are reversible by HDAC inhibition

Florian A. Siebzehnrübl[a,b,1], Kerstin A. Raber[c,1], Yvonne K. Urbach[c], Anja Schulze-Krebs[c], Fabio Canneva[c], Sandra Moceri[c], Johanna Habermeyer[c], Dalila Achoui[a], Bhavana Gupta[b], Dennis A. Steindler[a,d], Michael Stephan[e], Huu Phuc Nguyen[f,2], Michael Bonin[f,3], Olaf Riess[f], Andreas Bauer[g], Ludwig Aigner[h], Sebastian Couillard-Despres[i], Martin Arce Paucar[j], Per Svenningsson[j], Alexander Osmand[k], Alexander Andreew[l], Claus Zabel[l], Andreas Weiss[m], Rainer Kuhn[m], Saliha Moussaoui[m], Ines Blockx[n], Annemie Van der Linden[n], Rachel Y. Cheong[o], Laurent Roybon[p], Åsa Petersén[o], and Stephan von Hörsten[c,4]

[a]McKnight Brain Institute, Department of Neurosurgery, University of Florida, Gainesville, FL 32611; [b]European Cancer Stem Cell Research Institute, Cardiff University School of Biosciences, Cardiff CF10 3AX, United Kingdom; [c]Department of Experimental Therapy, Friedrich-Alexander-University, 91054 Erlangen, Germany; [d]Neuroscience and Aging Laboratory, Jean Mayer USDA Human Nutrition Research Center on Aging, Tufts University, Medford, MA 02155; [e]Clinic of Psychosomatic and Psychotherapy, Medical School Hannover, 30625 Hannover, Germany; [f]Institute of Medical Genetics and Applied Genomics, Center for Rare Diseases, University of Tübingen, 72074 Tübingen, Germany; [g]Institute of Neuroscience and Medicine, Forschungszentrum Jülich, 52425 Jülich, Germany; [h]Institute of Molecular Regenerative Medicine, Paracelsus Medical University, 5020 Salzburg, Austria; [i]Institute of Experimental Neuroregeneration, Spinal Cord Injury and Tissue Regeneration Center Salzburg, Paracelsus Medical University, 5020 Salzburg, Austria; [j]Section of Translational Neuropharmacology, Department of Physiology and Pharmacology, Karolinska Institute, 171 77 Solna, Sweden; [k]Department of Biochemistry and Cellular and Molecular Biology, University of Tennessee, Knoxville, TN 37996; [l]Institute for Human Genetics, Charité-Universitätsmedizin, 13353 Berlin, Germany; [m]Neuroscience Discovery, Novartis Pharma AG, 4056 Basel, Switzerland; [n]Bio-Imaging Laboratory, University of Antwerp, 2000 Antwerp, Belgium; [o]Translational Neuroendocrine Research Unit, Department of Experimental Medical Science, Lund University, 221 84 Lund, Sweden; and [p]Stem Cell Laboratory for CNS Disease Modeling, Department of Experimental Medical Science, Lund University, 221 84 Lund, Sweden

Huntington disease (HD) is an autosomal dominant neurodegenerative disorder caused by expanded CAG repeats in the *huntingtin* gene (*HTT*). Although mutant HTT is expressed during embryonic development and throughout life, clinical HD usually manifests later in adulthood. A number of studies document neurodevelopmental changes associated with mutant *HTT*, but whether these are reversible under therapy remains unclear. Here, we identify very early behavioral, molecular, and cellular changes in preweaning transgenic HD rats and mice. Reduced ultrasonic vocalization, loss of prepulse inhibition, and increased risk taking are accompanied by disturbances of dopaminergic regulation in vivo, reduced neuronal differentiation capacity in subventricular zone stem/progenitor cells, and impaired neuronal and oligodendrocyte differentiation of mouse embryo-derived neural stem cells in vitro. Interventional treatment of this early phenotype with the histone deacetylase inhibitor (HDACi) LBH589 led to significant improvement in behavioral changes and markers of dopaminergic neurotransmission and complete reversal of aberrant neuronal differentiation in vitro and in vivo. Our data support the notion that neurodevelopmental changes contribute to the prodromal phase of HD and that early, presymptomatic intervention using HDACi may represent a promising novel treatment approach for HD.

neurodegeneration | development | experimental therapy | animal model | multiomics

Pathological CAG repeat expansions in the human *Huntingtin* (*HTT*) gene on chromosome 4p16.3 cause autosomal dominant Huntington disease (HD), which is clinically characterized by the triad of chorea, cognitive dysfunction, and psychiatric symptoms (1, 2). After clinical onset the disease inevitably progresses, leading to severe disability and premature death with no effective disease-modifying treatments available.

The CNS pathology in advanced stages of HD is characterized by a loss of striatal medium spiny neurons (3) and cortical structures (4) as well as the presence of HTT$^+$ and ubiquitin$^+$ cytoplasmic and nuclear protein aggregates in neurons (5–7). The lengths of pathological CAG repeat expansions, which extend the polyglutamine stretch within HTT, correlate with earlier disease onset and greater severity (1, 8, 9). Over the past decades, the field has shifted from considering HD solely as a late-onset neurodegenerative disease: Instead HD is more recognized as a developmental disorder with various effects of mutant HTT (mHTT) on early neurodevelopment (10, 11).

HTT is expressed in preimplantation stages of the embryo (12, 13), and loss of HTT expression in mice is embryonic lethal (14–16), underlining its developmental importance. Several studies document mHTT-dependent changes during development, both

Significance

In Huntington disease (HD) gene carriers the disease-causing mutant *Huntingtin* (m*HTT*) is already present during early developmental stages but, surprisingly, HD patients develop clinical symptoms only many years later. While a developmental role of *Huntingtin* has been described, so far new therapeutic approaches targeting those early neurodevelopmental processes are lacking. Here, we show that behavioral, cellular, and molecular changes associated with m*HTT* in the postnatal period of genetic animal models of HD can be reverted using low-dose treatment with a histone deacetylation inhibitor. Our findings support a neurodevelopmental basis for HD and provide proof of concept that pre-HD symptoms, including aberrant neuronal differentiation, are reversible by early therapeutic intervention in vivo.

NEUROSCIENCE

in vivo and in stem cell-derived culture paradigms (11, 17–21). Specifically, mHTT affects striatal development in the Hdh-Q111 embryo (22), and conditional mHTT expression during development is sufficient to generate HD-like symptoms (23, 24). In animal models, early behavioral, cellular, and metabolic abnormalities are discernible in 4-wk-old tgHD rats and R6/2 mice, and changes in myelination were found in 14-d-old Hdh-Q250 mice (25–28). These studies indicate that HD pathology includes a neurodevelopmental phase that is present long before the onset of HD-like neurodegeneration and which not only contributes to the classical disease symptoms but is also likely to shape prodromal stages of HD.

In contrast to the later stages of symptomatic HD, prodromal manifestations are much less clearly defined. Previous studies indicate that emotional dysfunction and minor motor signs may precede the characteristic symptomatology (29, 30). Longitudinal studies of HD carriers aim to define the spectrum of early psychiatric symptoms in HD (29, 31). Additionally, differences in cranial volume and growth have been observed in young, presymptomatic gene carriers (32). Thus, the clinical and molecular delineation of the early stages of HD is a central issue in the implementation of future targeted treatment strategies and the identification of new biomarkers.

Here, we provide evidence that changes in neuronal differentiation continue postnatally in two mouse and rat HD animal models and that molecular, cellular, and behavioral alterations may be reversible through early therapeutic intervention with histone deacetylase inhibitors (HDACi). HDACi are promising compounds that are neuroprotective in HD mice (33), alleviate motor symptoms in the R6/2 model (34, 35), and were in clinical trials for HD (36).

A previous study showed that mHTT affects neural development pathways in HD-derived induced pluripotent stem cells (iPSCs) (21), and we extend these findings to the systems level, revealing cellular and behavioral correlates of neurodevelopmental gene-expression pathways. Importantly, these mHTT-induced changes are reversible by low-dose therapy with the histone deacetylase inhibitor LBH589 (Panobinostat), which restores neural differentiation phenotypes in vitro and in vivo.

Results

Transgenic Rodent HD Models Display a Postnatal Behavioral Phenotype with Decreased Anxiety. We began by investigating if the presence of mHTT in the developing CNS causes measurable changes in early postnatal HD animals. Therefore, we employed the earliest quantifiable behavioral assays and tested transgenic tgHD (51 CAG repeats, adult onset) and BACHD mouse (97 CAG repeats, juvenile onset) pups for emotional behavior (ultrasonic vocalization, USV) at postnatal day (P) 10, sensorimotor gating (prepulse inhibition, PPI) at P17, and risk-taking behavior [novel cage test, NCT (37)] at P21. USV analysis revealed a decreased number and shorter duration of ultrasonic calls from both tgHD rat and BACHD transgenic pups separated from their dam compared with WT littermates (Fig. 1 A and B), indicating changes in perception (reduced awareness), emotionality (reduced anxiety), and/or executive functions (reduced pattern to vocalize as an indicator of emotional and/or motor functions). We employed PPI to test for a reduction in sensorimotor gating and observed a loss of PPI in tgHD rats but not in BACHD mice (Fig. 1 C and D). In a test for anxiety and risk-taking behavior, transgenic pups from both models showed greater mobility and remained in the center area of a new cage for significantly longer durations than WT pups, suggesting reduced anxiety and increased risk-taking behavior (Fig. 1 E and F). These combined tests indicate decreased anxiety levels in early postnatal HD rodents. Fig. 1 G and H summarize the behavioral phenotypes of the tgHD rat model and the BACHD mouse model, respectively.
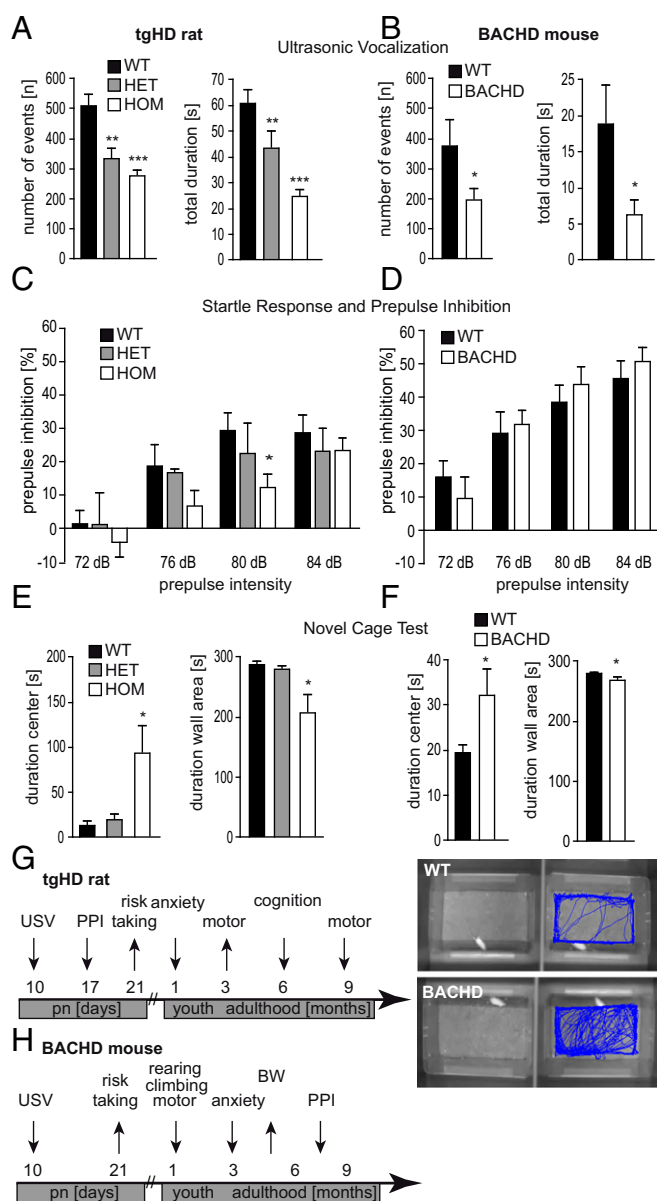

Fig. 1. Early behavioral phenotyping in transgenic models of Huntington disease. Rat (SPRDtgHD) and mouse (BACHD) pups were screened for a behavioral phenotype between P10 and P21. (A and B) The number and total duration of ultrasonic calls in WT, hemizygous (HET), and homozygous (HOM) rat pups (n > 30) (A) and WT and hemizygous (BACHD) mouse pups (n > 7) (B) were determined at P10. Transgenic pups emitted significantly fewer calls of shorter duration. (C and D) Startle response and PPI were measured at P17. Transgenic HD rat pups showed a significant loss of PPI at a prepulse of 80 dB white noise (n > 8) (C), while no differences were observed in BACHD mice at this age (n = 10) (D). (E and F) Altered exploration and risk behavior were detected in transgenic preweaning rats (E) as well as in transgenic mice at P21 (F) using the NCT. The time spent in the center of the cage was significantly increased in tgHD homozygous rat pups (n = 5) (E) and BACHD mouse pups (n = 8) (F), while the time spent in the wall area was significantly decreased. (G and H) A time-course graph illustrates the development of the behavioral phenotype of the transgenic tgHD rats (G) and BACHD mice (H). Data represent means ± SEM. Statistical analyses using ANOVA: *P < 0.05, **P < 0.01, and ***P < 0.001 vs. WT pups.

Dopaminergic and Glutamatergic Imbalance in Postnatal tgHD Rat Striatum. We then analyzed gene expression in the striatum of homozygous tgHD P10 rat pups and age-matched WT littermates using Affymetrix arrays to identify molecular changes that may be the underlying cause for the early behavioral symptoms. This

revealed a high number of differentially regulated genes (Fig. 2A and Dataset S1). Using the Ingenuity Pathway Analysis software to classify genes according to function, we identified 17 aberrantly regulated candidate genes associated with "behavior" (Fig. 2 B and C). qRT-PCR validation confirmed aberrant regulation of seven candidates: angiotensinogen (*Agt*), ATPase, Ca^{2+} transport (*Atp2A2*), Forkhead box G1B (*FoxG1B*), hypocretin (orexin) receptor (*Hcrtr2*), potassium channel, member 1 (*Kcnc1*), solute carrier family 6, 3 (dopamine transporter) (*Slc6A3*), and tyrosine hydroxylase (*Th*) (Fig. 2B). Since the two most up-regulated of these seven candidates were related to dopaminergic signaling (Fig. 2C), we analyzed striatal

dopaminergic circuits in more detail and further quantified the mRNA levels of DARPP-32, the dopamine receptor D1A, and protein kinase A (PKA) by qRT-PCR. In contrast to the observed up-regulation of *Slc6A3* and *Th*, we found that all three genes were significantly down-regulated in the striatum of tgHD P10 pups (Fig. 2D).

Western blot analyses of total protein extracts from striatal tissue at P10 confirmed significantly reduced protein levels of DARPP-32 (Fig. 2E). Of note, there was a trend toward increased phosphorylation at Thr^{75} and Thr^{34} in DARPP-32.

These studies were complemented by autoradiography for striatal expression of D1A, D2, NMDA, 5-HT2, adenosine A1,
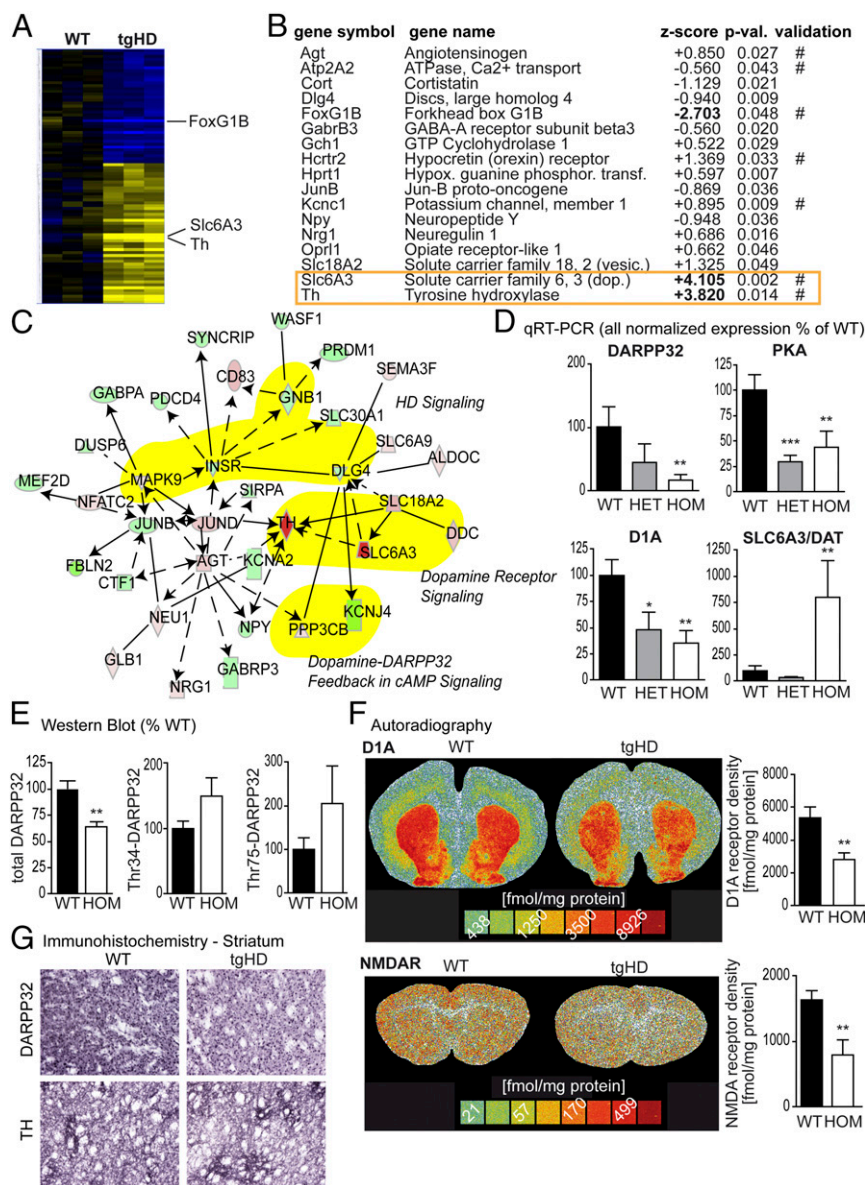

Fig. 2. Molecular analyses of tgHD P10 striata. (A) Microarray analysis of rat striata at P10 (WT vs. HOM, n = 5 each) demonstrated clusters of up- (yellow) and down- (blue) regulated gene expression. (B) Ingenuity Pathway Analysis revealed 17 target mRNAs associated with behavior, 7 of which (#) were validated by qRT-PCR (P values are from ANOVA vs. WT; n > 8). (C) Network analysis indicated deregulation of dopaminergic signaling; relevant pathways are highlighted in yellow). Rat P10 striatal mRNA expression of DARPP-32, PKA, and dopamine receptor D1A is down-regulated, whereas the expression of the dopamine transporter Slc6a3 is up-regulated. (D) Data are displayed as mean normalized expression (percentage of WT; ANOVA; n > 8). (E) DARPP-32 down-regulation two-tailed t test; n > 5) could be confirmed in Western blot studies. Phosphorylation levels of DARPP-32 (Thr^{34} and Thr^{75}) in P10 striata were not significantly different in WT and transgenic pups. (F) Receptor autoradiography revealed a significant reduction of dopamine receptor D1A density and NMDAR density in the striata of transgenic rat pups (two-tailed t test; n = 5). Representative autoradiographs of coronal sections of P10 rats are presented. (G) Immunohistochemistry confirmed the reduced expression of DARPP32 and TH in the striatum of P10 tgHD pups (shown are representative images from n = 10 pups). Data represent means ± SEM: *P < 0.05, **P < 0.01, and ***P < 0.001 vs. WT pups.

and adenosine A2A receptors in P10 rat pups. We found decreased levels of the dopaminergic receptor D1A (Fig. 2F) and NMDA receptor (NMDAR) density (Fig. 2F and *SI Appendix*, Fig. S1A). Further Western blot analyses of NMDAR subunits revealed down-regulation of NR1, NR2B, and NR2C (*SI Appendix*, Fig. S1B). Immunohistochemical analysis of P10 tgHD striata confirmed reduced expression of DARPP32 and TH (Fig. 1G).

As mRNA expression changes do not always translate into altered protein levels, and because other regulatory mechanisms may also affect protein synthesis, we performed proteomic analysis using 2D electrophoresis and subsequent MALDI-TOF of P10 pup striata as well. In the R6/2 model, large-scale alterations of protein levels precede the onset of classical symptoms (38). Similarly, we found 156 proteins to be significantly altered in pre-HD tgHD rat brains. These could be classified into six Kyoto Encyclopedia of Genes and Genomes (KEGG) pathways, confirming the observed alterations in metabolic pathways (38) and further identifying changes in axon sprouting and neurodegenerative pathways (Dataset S2). These studies revealed an additional down-regulated regulatory subunit of protein phosphatase 1 (PPP1R7) (39, 40). Taken together, these data reveal imbalances in dopaminergic and glutamatergic pathways in the early postnatal period of tgHD rats sufficient to explain the behavioral phenotype.

Altered Neuronal and Oligodendroglial Differentiation Capacity in HD.

Olfactory dysfunction is among the earliest discernible symptoms in neurodegenerative diseases, including Parkinson, Alzheimer, and Huntington disease (41). Because of the well-established link between subventricular zone (SVZ) neurogenesis and the olfactory system, the observed association of aberrant SVZ neurogenesis and olfactory dysfunction in neurodegenerative diseases (42), the reported regulatory functions of dopaminergic and glutamatergic signaling for neurogenesis (43), and the potential implications of the olfactory system for our observations of animal behavior, we investigated SVZ neurogenesis in our model.

While neurodegeneration is characteristic of HD, previous studies observed aberrant neuronal differentiation during embryonic development in vitro and in vivo in the Hdh-Q111 model (22, 23), as well as in iPSC-derived neural precursors from HD patients (21). Therefore it is likely that any aberrations on the cellular and molecular level underlying behavioral changes are the product of aberrant neurodevelopmental rather than neurodegenerative processes. Consequently, we asked whether mHTT affected neuronal differentiation capacities of SVZ neural stem/progenitor cells (NSCs) during postnatal development. We cultured NSCs from P10 WT, tgHD$^{+/-}$, and tgHD$^{+/+}$ pups and differentiated them into glial and neuronal lineages. This resulted in a significant, gene dose-dependent reduction in neuronal numbers at all time points (Fig. 3 A–C). Analysis of differentiation to mature neuronal phenotypes revealed a reduction in bIII tubulin$^+$ neurons at 7 d in vitro (DIV) (Fig. 3B), as well as lower numbers of NeuN$^+$ neurons at 14 and 28 DIV (Fig. 3B). Likewise, Darpp32$^+$ cell numbers were reduced in tgHD$^{+/+}$ cultures at 14 and 28 DIV, while we observed an increase at 14 DIV and a decrease at 28 DIV in tgHD$^{+/-}$ cultures (Fig. 3C). Astrocyte numbers were unchanged, but oligodendrocyte counts were significantly increased after differentiation (Fig. 3 A and B). These findings demonstrate an increase in oligodendroglial differentiation at the expense of neuron production from SVZ-derived NSC cultures in heterozygous and homozygous tgHD pups. Differentiation of tgHD cultures was accompanied by an increase in apoptotic cells identified by active caspase 3 staining. This is also reflected in reduced total cell counts in tgHD$^{+/-}$ and tgHD$^{+/+}$ cultures compared with WT cultures (Fig. 3D).

To determine if neuronal, oligodendroglial, and glial differentiation capacity was also affected in BACHD mice, we generated neurospheres from BACHD and WT littermates at E13.5. We detected significant reductions in the total number of cells, MAP2-immunopositive neurons, and 2′3′-cyclic-nucleotide 3′-phosphodiesterase (CNPase)-immunopositive oligodendrocytes in BACHD cultures compared with WT cultures at 7 DIV, while astrocyte numbers remained unchanged (Fig. 3E).

Because of the profound changes in differentiation capacity between WT and tgHD NSC cultures, we were interested in whether in vivo neurogenesis was affected by the presence of mHTT. To address this, we crossbred tgHD rats with a model expressing the reporter dsRed2 under control of the Dcx promoter (dcx::dsRed2,tgHD) (44). Dcx is a marker of newborn, migratory neurons and is expressed up to 14 d after the birth of new neurons (45). We analyzed sagittal sections of dsRed2$^+$ WT and tgHD pups, revealing minor differences in rostral migratory stream (RMS) and olfactory bulb (OB) volumes and a significant reduction in the content of Dcx$^+$ neurons (proportional to the relative fluorescence intensity; see heatmaps in Fig. 3F). This corroborates the reduced capacity for SVZ neurogenesis in the tgHD model.

Of note, diffusion tensor imaging (46) revealed a trend toward an increase in axial diffusivity, radial diffusivity, and mean diffusivity and a reduction in fractional anisotropy in tgHD pups compared with WT pups (*SI Appendix*, Fig. S1C).

Low-Dose LBH589 Treatment Restores the Early Behavioral, Cellular, and Molecular Phenotype in HD.

The observed mHTT-associated aberrations at the molecular, cellular, and behavioral levels in these HD models extend previously reported alterations in embryonic development to the early postnatal phase, a time of neuronal maturation and gliogenesis. We next tested whether therapeutic intervention can restore these changes.

HDACi have a long history of use for their mood-stabilizing and antiepileptic effects. In models of HD, previous studies have demonstrated that the HDACi SAHA (Vorinostat) could reverse motor symptoms and improve phenotypes in the R6/2 model (34, 35). Because of the neuroprotective effects of LBH589 in mouse models of HD (33) and its ability to cross the blood–brain barrier (Dataset S3) (47), we treated tgHD pups with this HDACi. TgHD rat pups and WT littermates were subjected to four different dose regiments, administered every other day between P8 and P20 (Fig. 4A and *SI Appendix*, Fig. S2 A and B). We analyzed USV at P11, startle response and PPI at P17, and the NCT at P21. Administration of 0.001 mg/kg LBH589 led to significantly increased USV in transgenic rat pups (Fig. 4B). LBH589 had a suppressive effect on PPI and startle response independent of the individual genotype at all doses (Fig. 4C). In addition, performance in the NCT was improved in tgHD rats: Duration in the center was reduced, and duration in the wall areas increased to match values of vehicle-treated WT animals (Fig. 4D). In contrast, LBH589 had no effect on WT animals in this test. Furthermore, the average velocity and track length in tgHD pups were restored to WT levels (*SI Appendix*, Fig. S2A), while in the 0.01 mg/kg WT group the average velocity and track length were significantly decreased compared with vehicle-treated WT animals. The improved performance of LBH589-treated tgHD pups in USV and NCT tests indicates that this compound alleviates the reduced anxiety and increases risk-taking behavior in these animals.

We have previously demonstrated that HDACi increase the neuronal differentiation capacities of NSCs (48). Therefore, we tested whether exposure to LBH589 could restore neuronal differentiation of tgHD NSCs in vitro. After testing for optimal dose regimens (*SI Appendix*, Fig. S2C), we found that treatment of differentiating NSC cultures with 10 nM LBH589 for 24 h restored neuronal differentiation of tgHD cultures to WT levels.
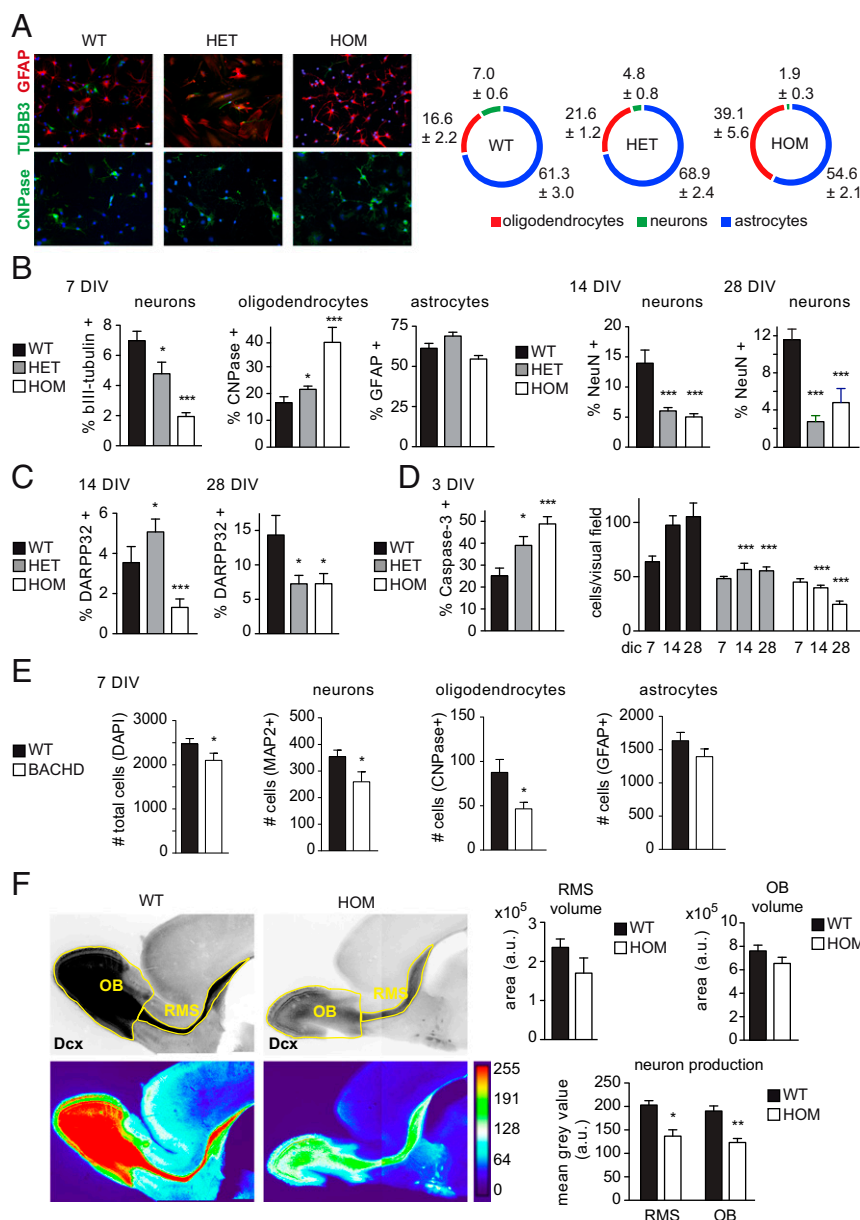
Fig. 3. (*A, Left*) Cellular analysis of tgHD P10 neurogenesis. Quantitative analysis of P10 rat neurosphere differentiation demonstrated reduced neuronal (bIII tubulin, green, *Upper*) and increased oligodendroglial (CNP, green, *Lower*) differentiation, while astroglial (GFAP, red, *Upper*) fates were unaffected (Scale bar, 20 μm applies to all images.). (*Right*) Graphical representation indicates percentages ± SEM of individual cell types. (*B*) After 7 d in vitro (DIV) differentiation, neuron numbers were significantly decreased, while oligodendrocyte counts were increased. Astrocyte numbers were not affected significantly. Numbers of mature, NeuN-expressing neurons were significantly reduced at 14 DIV and 28 DIV. (*C*) Similarly, DARPP32$^+$ cell counts were significantly reduced at both time points. (*D*) The differentiation phenotype was accompanied by an increase in apoptosis, which is reflected in lower cell counts after differentiation. In *A–D*: ANOVA; $n = 3$ independent experiments with 10 replicates. (*E*) Differentiation of BACHD embryonic (E13.5) neurospheres revealed significantly lower numbers of total cells and MAP2$^+$ and CNPase$^+$ cells compared with WT cultures (ANOVA; $n = 8$). GFAP$^+$ astrocyte counts were unchanged. (*F*) In vivo changes in neuronal differentiation are reflected in the RMS and OB of P10 Dcx-dsRed2-tgHD double transgenic pups (Mann–Whitney *U* test, $n = 7$). (*Upper Left*) Inverted fluorescence images. (*Lower Left*) Heatmaps of fluorescence intensity. (*Right*) While the volume of RMS and OB was not significantly different, the mean fluorescence intensity (proportional to neuronal numbers) was significantly reduced in both structures. Data represent means ± SEM. *$P < 0.05$; **$P < 0.01$; ***$P < 0.001$.

Comparing bIII tubulin$^+$ cells at 7 DIV and NeuN$^+$ and Darpp32$^+$ cells at 14 DIV, we observed a significant increase in neurons at all time points (Fig. 4*E*), indicating improved regenerative capacities of SVZ stem/progenitor cells after treatment. LBH589 treatment had no effect on total cell numbers in WT controls but increased tgHD total cell numbers (Fig. 4*F*).

Similarly, treatment of E13.5-derived BACHD NSC cultures with 10 nM LBH589 increased the percentage of MAP2$^+$ neurons in both WT and BACHD cultures at 7 DIV (Fig. 4*G*).

LBH589 exerted a positive effect in WT cultures at 1 nM, whereas BACHD cultures required 10 nM to increase the percentage of MAP2 cells. Furthermore, treatment increased the percentage of CNPase$^+$ oligodendrocytes at 7 DIV. There were no differences in GFAP$^+$ astrocyte numbers between any treatment conditions in BACHD and WT cultures (*SI Appendix*, Fig. S2 *D–G*).

Transcriptomic and proteomic profiling (Fig. 2, *SI Appendix*, Fig. S3, and Dataset S2) identified alterations in several pathways relevant to HD pathogenesis and neurodevelopment (*SI*
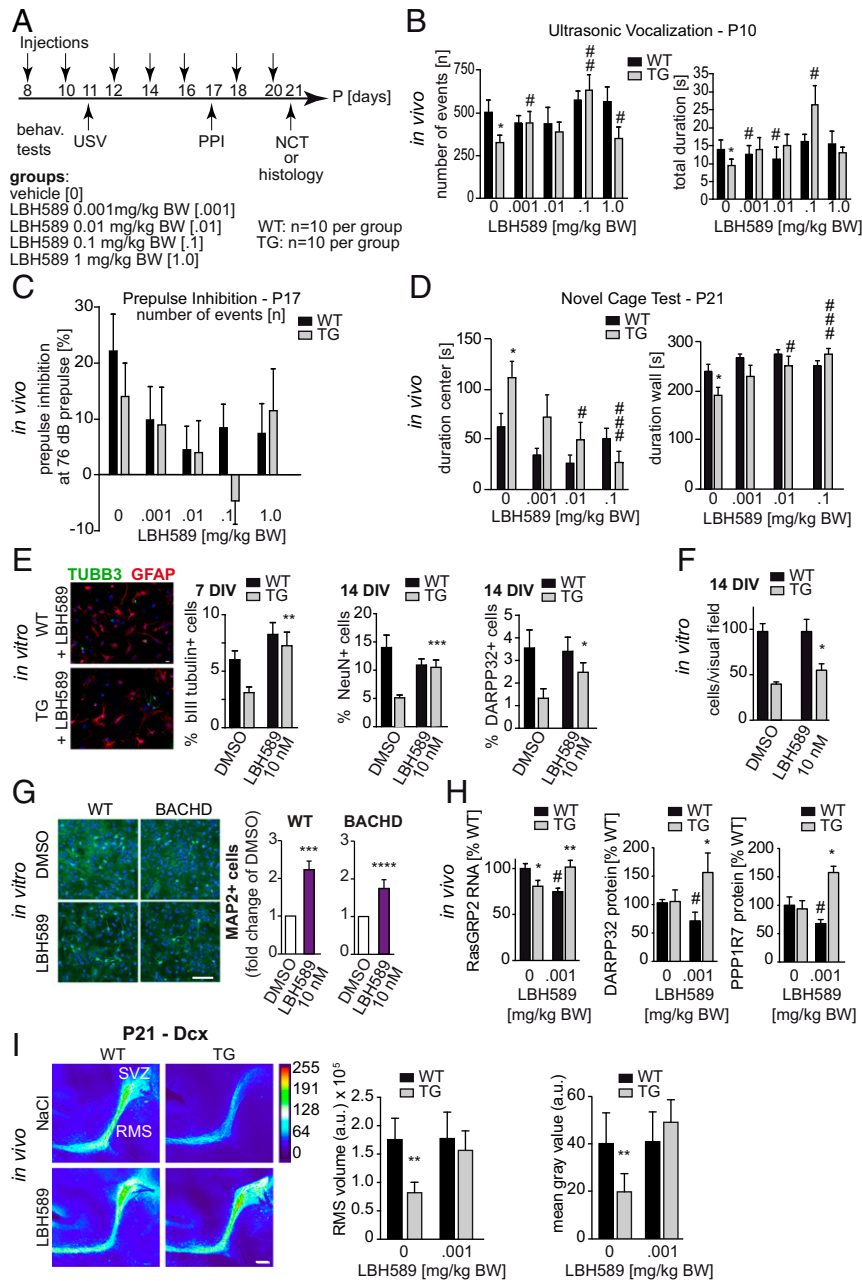
Fig. 4. (*A*) Treatment of early phenotype using HDAC inhibitor LBH589. tgHD HOM pups and WT controls were treated with the HDACi LBH589 from P8 to P20 (*n* = 10 each). Behavioral readouts were USV (P11), startle response and PPI (P17), and NCT (P21). Four different doses (0.001, 0.01, 0.1, and 1.0 mg/kg body weight) were administered i.p. every other day. (*B*) The numbers of ultrasonic calls were significantly increased in transgenic animals treated with LBH589 compared with vehicle controls. The increase in the total duration in transgenic animals did not reach significance except for the 0.1 mg/kg group (0.001 mg/kg: *P* = 0.2561; 0.01 mg/kg: *P* = 0.1949; 0.1 mg/kg: *P* = 0.0016; ANOVA; *n* > 10). (*C*) PPI was suppressed in animals treated with LBH589 in all doses tested compared with WT (ANOVA; *n* > 3). (*D*) LBH589 treatment significantly decreased the time spent in center areas and increased the time spent in wall areas in transgenic rats compared with corresponding vehicle-treated transgenic animals (ANOVA; *n* > 4). LBH589 had no significant effect on WT animals. (*E*) LBH589 treatment of differentiating neurosphere cultures restored tgHD HOM neuron numbers to WT levels. Shown are representative images of cultures treated with 10 nM LBH589 for 24 h. (Scale bar, 20 μm in both images.) TuJ^{+} neurons were counted after 7 d, and NeuN[+] and Darpp32^{+} neurons were quantified after 14 d. TuJ[+], NeuN[+], and Darpp32^{+} cells were within the range of WT cultures (ANOVA; *n* = 3 independent experiments with 10 replicates). (*F*) LBH589 treatment resulted in increased cell counts in transgenic but not in WT cell cultures. (*G, Right*) The percentage of MAP2-immunopositive neurons was significantly increased with 10 nM LBH589 in WT and BACHD E13.5 neurosphere cultures (ANOVA; *n* = 8). (*Left*) A representative photomicrograph showing MAP2^{+} neurons (green) and DAPI (blue) from WT and BACHD cultures. (Scale bar, 100 μm.) (*H*) LBH589 treatment (0.001 mg/kg) increased striatal *RasGRP2* gene expression and DARPP32 and PPP1R7 protein levels in P10 tgHD pups but not in WT littermates (ANOVA; *n* > 6). (*I, Left*) Heatmaps of dcx-stained immunofluorescence micrographs from P21 tgHD pups highlight SVZ–RMS neurogenesis in vivo. (Scale bar, 100 μm.). (*Right*) LBH589 treatment restored both RMS volume and dcx fluorescence intensity in tgHD pups to WT levels (seven injections of 0.001 mg/kg compared with vehicle control; two-way ANOVA; *n* > 3). Data represent means ± SEM. Significant effects vs. WT (**P* < 0.05; ***P* < 0.01; ****P* < 0.001; *****P* < 0.0001) and treatment effects vs. vehicle control (#*P* < 0.05; ##*P* < 0.01; ###*P* < 0.001).

Appendix, Fig. S4). We therefore tested whether in vivo LBH589 treatment affected expression of a target gene of the dopamine pathway in medium spiny neurons (RasGRP2), which is down-regulated in HD (49). LBH589 treatment increased RasGRP2 expression and restored protein levels of two additional markers of striatal development, DARPP-32 and PPP1R7 (Fig. 4*H* and *SI Appendix*, Fig. S5).

To determine whether LBH589 was capable of restoring neurogenesis in vivo, we quantified RMS volume and Dcx staining intensity in vehicle- and LBH589-treated WT and tgHD pups at P21. Continuous administration of 0.001 mg/kg LBH589 from P8 to P20 (seven doses) could restore in vivo neuronal differentiation and neurogenesis in tgHD pups to WT levels (Fig. 4*I*).

Thus, early postnatal behavioral, cellular, and molecular alterations of HD can be alleviated by low-dose therapy with LBH589.

Discussion

Here we describe behavioral, cellular, and molecular changes during a developmental phase of gliogenesis and neuronal maturation that is comparable to the third trimester of human gestation (50). Importantly, these changes can be reversed by treatment with HDACi, which fully restores alterations in neuronal differentiation in HD pups. Hence, these data contribute to the increasing evidence of neurodevelopmental aberrations in genetic animal models of HD and suggest that HD should be considered a neurodevelopmental disorder.

We identify reduced separation-induced USV at P10 and increased risk-taking behavior at P21 as key features of an early behavioral phenotype in transgenic HD mice and rats. These features may correspond to an anxiolytic phenotype similar to the reduced anxiety-like behavior found in transgenic HD rats at 1 mo of age (26) or may be attributable to depression-like features as described in 2-mo-old BACHD mice (51). Dopaminergic and glutamatergic signaling regulate neuronal differentiation during development, and deregulation of these pathways may provide a molecular basis for HD-associated behavioral changes. These species-independent behavioral abnormalities provide a readout for the prodromal phase of HD, which is characterized by neurodevelopmental rather than neurodegenerative mechanisms. mHTT causes aberrant neuronal differentiation during embryonic development and from iPSCs (21–24). Our findings link alterations in neuronal differentiation and molecular pathways to behavior on the systems level.

These observations support the notion that HD pathology consists of at least three phases: (*i*) an early phase with successful adaptation to the effects of accumulating mutant Htt, likely to be outbalanced by changes in early neurodevelopment. This early phenotype presents with signs of overcompensation and is followed by an intermediate and largely silent phase, which, depending on the number of CAG repeats at mid-age, shifts into a third phase of overt decompensation and neurodegeneration. The notion that this early phase of HD may be viewed as a slowly progressive neurodevelopmental disorder that ultimately transforms into a neurodegenerative disease is documented in many studies identifying symptoms long before the onset of neurodegeneration in animal models (25–28, 52). In view of this evidence for a "pre-HD syndrome," it should be mentioned that such changes may not be "disease-like" but instead may reflect a whole spectrum of signs and symptoms attributable to higher glutamine availability in the CNS and/or successful compensation and repair of the very early damage associated with mHTT. The former would be in line with the hypothesis of polyglutamine diseases arising from evolutionary search mechanisms (53) attempting to increase central glutamine storage in the brain, while the latter would imply that neurotrophic factors are induced, which may affect development in all its dimensions of growth, maturation, and learning. Whether mHTT causes developmental aberrations in gene carriers is still unclear, but re-

cent studies have found differences in growth and development as well as in cranial volume in both adult (32) and juvenile (54) premanifest gene carriers.

Microarray analyses detected deregulation of the dopamine-signaling pathway in postnatal tgHD rats. This was corroborated by findings of deficits in the D1/cAMP/PKA/DARPP-32 signaling cascade of P10 tgHD rats. These findings in the postnatal tgHD rat brain mirror previous imaging studies in asymptomatic HD gene carriers (55, 56), which revealed a reduction of striatal D1 and D2 receptors. Evidence of dopaminergic deregulation and receptor imbalance has been further substantiated in molecular studies of postmortem HD brains (57–59) and imaging studies of symptomatic HD patients (60, 61). Previous studies in 4-wk-old HD mice also demonstrated a reduction of total levels of DARPP-32 and D1 receptor protein levels (62). We previously showed that a significant loss of striatal D1 receptor expression and DARPP-32$^+$ cells is present in 14-mo-old male tgHD animals. Beyond deregulation of dopaminergic-signaling pathways, we observed significantly reduced NMDAR density in the striatum of tgHD P10 rat pups. NMDAR numbers are reduced, particularly in the basal ganglia, in both symptomatic (63, 64) and presymptomatic (65) HD patients. Early changes in extrasynaptic NMDAR signaling and expression have also been reported in 1-mo-old pre-symptomatic YAC72 and YAC128 mice before the onset of motor dysfunction and neuronal loss (66). Furthermore, there is evidence indicating that mHTT increases NR2B-containing extrasynaptic NMDARs in the striatum of young YAC72 and YAC128 mice (67). By contrast, our own data in P10 rat tissue show a down-regulation of the NR1, NR2B, and NR2C subunits of NMDARs. A pathogenic link between dopamine and glutamate signaling is provided by studies showing that striatal dopamine modulates ionotropic glutamate receptors by altering glutamate currents and by modifying glutamate receptor surface localization (68, 69). Since D1 receptors and NMDARs are capable of direct interaction, which affects receptor activity (70), it is possible that the aberrant striatal receptor expression observed in P10 tgHD rats is due to abnormal glutamate/dopamine receptor interactions. Alternatively, down-regulation of D1A receptors and NMDARs could also suggest a developmental delay in tgHD pups.

SVZ neurogenesis has been shown to affect social behavior (71), and aberrations in olfaction and SVZ neurogenesis are among the earliest symptoms in neurodegenerative diseases (41, 42). SVZ neurogenesis is modulated by dopamine and glutamate (43); thus it is likely that the observed deregulation of both pathways extends to neural stem cells as well. We demonstrate that SVZ-derived NSC cultures show a prominent reduction of their neuronal differentiation in both tgHD and BACHD models, which is corroborated by a reduction of NeuN$^+$ neurons at 14 and 28 DIV in tgHD. The different results in oligodendrocyte differentiation between tgHD and BACHD models may be explained by their different ages at isolation. Oligodendroglial maturation and myelination start around P14 in vivo; thus embryonic-derived BACHD cultures may be too early to reflect mHtt effects on the oligodendrocyte lineage. Altered SVZ neurogenesis could be confirmed in vivo in P10 tgHD rats. Others have shown the relevance of mHTT during development (22, 23) as well as its impact on the differentiation capacities of pluripotent SC-derived neural precursors (21, 72). mHTT has been shown to affect the proliferation and cell fate of cortical progenitor cells (18). Consequently, the reduced neuronal differentiation observed here is likely due to direct effects of mHTT in neural precursors.

Bystander microenvironmental effects, e.g., from microglia, may contribute as well, as it has been shown that these cells affect SVZ neurogenesis in vitro (73). The specific effects of mHTT on postnatal neurogenesis in symptomatic HD models are somewhat controversial. While some studies did not find changes in SVZ proliferation or differentiation in R6/2 or YAC128 mice (74, 75), others detected reduced levels of neurogenesis in the R6/2 model

(76, 77) and aberrant neuronal differentiation in tgHD rats (78). In HD patients, cell proliferation in the SVZ is increased, which correlates with disease grade (79). Importantly, our observations are made long before the onset of classical symptoms. Thus, it is conceivable that mHTT reduces the generation of new neurons during earlier stages, while SVZ cell proliferation as a reaction to neurodegenerative processes dominates later stages of the disease.

Reduced neurogenesis may ultimately contribute to disease progression, i.e., lack of regeneration of striatal cell loss and dysfunction. This hypothesis is further supported by the observation of reduced numbers of striatal neurons (80) and reduced numbers of medium spiny neurons (81) in the tgHD rat model.

Transcriptional deregulation is known to be part of the pathogenesis of HD (82, 83). A number of studies showed that HDACi ameliorate neurodegeneration in cell systems and fly models (84) as well as motor deficits in a mouse model of HD (34, 85). Here we treated postnatal tgHD rats with the HDACi LBH589 (86) to intervene with neurodevelopmental changes in a preclinical setting. LBH589 is known to cross the blood–brain barrier efficiently and has already been tested in preclinical studies (33, 47). Low-dose treatment with LBH589 led to a partial reversal of behavioral symptoms and restored aberrant neuronal differentiation in tgHD and BACHD cultures in vitro and in tgHD pups in vivo. We conclude that very early LBH589 treatment may be a promising treatment approach in HD.

Methods

Animals. We used several tgHD litters derived from mating male and female tgHD$^{+/-}$ rats carrying a truncated human *HTT* fragment of 51 CAG repeats under control of the native rat HTT promoter (87). BACHD mouse pups were derived from mating hemizygous male BACHD mice (expressing floxed *HTT* with 97 CAG repeats) with female FVB/N dams (88). All animal experiments presented here were approved by local ethical boards of the District Government of Middle Franconia, Bavaria, Germany (approval no. 54-2532.1-16/08) and the University of Florida Institutional Animal Care and Use Committee, and were conducted according to local, NIH, and ARRIVE guidelines (89).

Behavioral Phenotyping.

USV. P10 rat and mouse pups were placed into a recording cage in a sound-isolation box. The detection sessions were initiated directly thereafter and were always performed by the same experienced experimenter between 8 and 10 AM. A maximum of two pups per litter were tested for 5 min each. For P10 rats and mice signals were recorded at a 35–250 kHz range using an Avisoft Ultra Sound Gate 116Hb (Avisoft Bioacoustics). Incoming signals were displayed as a time–event plot by Avisoft recorder software. For further statistical analysis, the parameters number of events (*n*) and total duration of cues (*s*) were analyzed using one-way ANOVA.

Acoustic startle response and PPI. Startle response and PPI were measured in homozygous ($^{+/+}$; $n \geq 10$), hemizygous ($^{+/-}$; $n \geq 10$), and WT ($^{-/-}$; $n \geq 10$) tgHD rats and hemizygous ($^{+/-}$; $n \geq 10$) and WT ($^{-/-}$; $n \geq 10$) BACHD mice at P17. The test point was validated in preliminary experiments. Pups were placed in a startle chamber, and the protocol was conducted as described previously

(90). Results were analyzed using one-way ANOVA and are displayed as the percentage of startle-response inhibition.

NCT. The NCT was performed in P21 preweaning homozygous ($^{+/+}$; $n \geq 5$), hemizygous ($^{+/-}$; $n \geq 5$), and WT pups analyzed using one-way ANOVA.

Treatment with HDACi LBH589. Pups were genotyped 3 d after birth, divided into groups of 10 according to genotype, and marked daily throughout the experiment. The animals were treated with LBH589 (Novartis) using the following doses: 0.001 mg salt/kg body weight, 0.01 mg salt/kg body weight, 0.1 mg salt/kg body weight, and 1 mg salt/kg body weight. Control animals were treated with vehicle: 0.03 M lactic acid/5% dextrose in water buffered to pH 4.2–4.5 with 0.1 M NaOH. LBH589 was administered i.p. every 48 h from P8 to P20. The behavioral tests were performed at P11 (USV), P17 (startle response and PPI), and P21 (NCT). Pups were killed at day 21 for histology.

Double-Transgenic Model and in Vivo Neurogenesis. tgHD rats were crossbred with a rat model expressing dsRed2 under control of the dcx promoter (Dcx::dsRed2) (91). The resulting offspring were interbred to generate hemizygous tgHD rats that were either homozygous or WT for dcx-dsRed2 (tgHD$^{+/-}$ dsRed2$^{-/-}$ or tgHD$^{+/-}$ dsRed2$^{+/+}$). Interbreeding these animals generated tgHD WT and homozygous offspring that were heterozygous for dcx-dsRed2 (tgHD$^{-/-}$ dsRed$^{+/-}$ or tgHD$^{+/+}$ dsRed2$^{+/-}$). Animals from these litters were genotyped at P3 and were used for experiments at P10. Pups were anesthetized on ice and then were transcardially perfused using 4% paraformaldehyde (PFA), and their brains were removed and postfixed in 4% PFA overnight. Fixed brains were washed twice in PBS and then were sectioned at 100 microns in the sagittal plane on a Leica VT-1000S vibratome. Serial sections from one hemisphere were mounted onto glass slides, air-dried, and coverslipped using VECTASHIELD with DAPI (Vector Laboratories). Low-power fluorescent images were taken on a Leica DMLB epifluorescence microscope equipped with a CCD camera (Spot Imaging Solutions). To obtain full images of brain sections, multiple gray-scale images were acquired per section using Spot Advanced software (Spot Imaging Solutions) and were merged into a full image and inverted into black-on-white images using Photoshop CS4 (Adobe Systems). Merged images were imported into ImageJ (NIH), and area size and mean pixel values of RMS and OB were analyzed.

Data Analysis. All data were analyzed with GraphPad Prizm 7.0 (GraphPad Software), and statistical significance was determined using appropriate statistical tests, as indicated in the figure legends. A *P* value of < 0.05 was deemed significant for all analyses. We used the D'Agostino–Pearson method to test for normal distribution of data points.

Additional methods are listed in *SI Appendix*.

1. The Huntington's Disease Collaborative Research Group (1993) A novel gene containing a trinucleotide repeat that is expanded and unstable on Huntington's disease chromosomes. *Cell* 72:971–983.
2. Paulsen J (1999) *Understanding Behavior in Huntington's Disease* (Huntington's Disease Society of America, New York).
3. Reiner A, et al. (1988) Differential loss of striatal projection neurons in Huntington disease. *Proc Natl Acad Sci USA* 85:5733–5737.
4. Rosas HD, et al. (2003) Evidence for more widespread cerebral pathology in early HD: An MRI-based morphometric analysis. *Neurology* 60:1615–1620.
5. Davies SW, et al. (1997) Formation of neuronal intranuclear inclusions underlies the neurological dysfunction in mice transgenic for the HD mutation. *Cell* 90:537–548.
6. DiFiglia M, et al. (1997) Aggregation of huntingtin in neuronal intranuclear inclusions and dystrophic neurites in brain. *Science* 277:1990–1993.
7. Martindale D, et al. (1998) Length of huntingtin and its polyglutamine tract influences localization and frequency of intracellular aggregates. *Nat Genet* 18:150–154.
8. Andrew SE, et al. (1993) The relationship between trinucleotide (CAG) repeat length and clinical features of Huntington's disease. *Nat Genet* 4:398–403.
9. Rubinsztein DC, Barton DE, Davison BC, Ferguson-Smith MA (1993) Analysis of the huntingtin gene reveals a trinucleotide-length polymorphism in the region of the

gene that contains two CCG-rich stretches and a correlation between decreased age of onset of Huntington's disease and CAG repeat number. *Hum Mol Genet* 2:1713–1715.
10. Humbert S (2010) Is Huntington disease a developmental disorder? *EMBO Rep* 11:899.
11. Wiatr K, Szlachcic WJ, Trzeciak M, Figlerowicz M, Figiel M (2018) Huntingon disease as a neurodevelopmental disorder and early signs of the disease in stem cells. *Mol Neurobiol* 55:3351–3371.
12. Bhide PG, et al. (1996) Expression of normal and mutant huntingtin in the developing brain. *J Neurosci* 16:5523–5535.
13. Jeong SJ, et al. (2006) Huntingtin is localized in the nucleus during preimplanatation embryo development in mice. *Int J Dev Neurosci* 24:81–85.
14. Duyao MP, et al. (1995) Inactivation of the mouse Huntington's disease gene homolog Hdh. *Science* 269:407–410.
15. Nasir J, et al. (1995) Targeted disruption of the Huntington's disease gene results in embryonic lethality and behavioral and morphological changes in heterozygotes. *Cell* 81:811–823.
16. Zeitlin S, Liu JP, Chapman DL, Papaioannou VE, Efstratiadis A (1995) Increased apoptosis and early embryonic lethality in mice nullizygous for the Huntington's disease gene homologue. *Nat Genet* 11:155–163.
17. Conforti P, et al. (2018) Faulty neuronal determination and cell polarization are reverted by modulating HD early phenotypes. *Proc Natl Acad Sci USA* 115:E762–E771.

18. Molina-Calavita M, et al. (2014) Mutant huntingtin affects cortical progenitor cell division and development of the mouse neocortex. *J Neurosci* 34:10034–10040.

19. Saudou F, Humbert S (2016) The biology of huntingtin. *Neuron* 89:910–926.

20. Raymond LA, et al. (2011) Pathophysiology of Huntington's disease: Time-dependent alterations in synaptic and receptor function. *Neuroscience* 198:252–273.

21. HD iPSC Consortium (2017) Developmental alterations in Huntington's disease neural cells and pharmacological rescue in cells and mice. *Nat Neurosci* 20:648–660.

22. Molero AE, et al. (2009) Impairment of developmental stem cell-mediated striatal neurogenesis and pluripotency genes in a knock-in model of Huntington's disease. *Proc Natl Acad Sci USA* 106:21900–21905.

23. Molero AE, et al. (2016) Selective expression of mutant huntingtin during development recapitulates characteristic features of Huntington's disease. *Proc Natl Acad Sci USA* 113:5736–5741.

24. Arteaga-Bracho EE, et al. (2016) Postnatal and adult consequences of loss of huntingtin during development: Implications for Huntington's disease. *Neurobiol Dis* 96:144–155.

25. Hickey MA, Gallant K, Gross GG, Levine MS, Chesselet MF (2005) Early behavioral deficits in R6/2 mice suitable for use in preclinical drug testing. *Neurobiol Dis* 20:1–11.

26. Nguyen HP, et al. (2006) Behavioral abnormalities precede neuropathological markers in rats transgenic for Huntington's disease. *Hum Mol Genet* 15:3177–3194.

27. Mochel F, et al. (2012) Early alterations of brain cellular energy homeostasis in Huntington disease models. *J Biol Chem* 287:1361–1370.

28. Jin J, et al. (2015) Early white matter abnormalities, progressive brain pathology and motor deficits in a novel knock-in mouse model of Huntington's disease. *Hum Mol Genet* 24:2508–2527.

29. Duff K, Paulsen JS, Beglinger LJ, Langbehn DR, Stout JC; Predict-HD Investigators of the Huntington Study Group (2007) Psychiatric symptoms in Huntington's disease before diagnosis: The predict-HD study. *Biol Psychiatry* 62:1341–1346.

30. Penney JB, Jr, et al. (1990) Huntington's disease in Venezuela: 7 years of follow-up on symptomatic and asymptomatic individuals. *Mov Disord* 5:93–99.

31. Paulsen JS, et al.; Predict-HD Investigators and Coordinators of the Huntington Study Group (2008) Detection of Huntington's disease decades before diagnosis: The predict-HD study. *J Neurol Neurosurg Psychiatry* 79:874–880.

32. Nopoulos PC, et al.; PREDICT-HD Investigators and Coordinators of the Huntington Study Group (2011) Smaller intracranial volume in prodromal Huntington's disease: Evidence for abnormal neurodevelopment. *Brain* 134:137–142.

33. Chopra V, et al. (2016) LBH589, a hydroxamic acid-derived HDAC inhibitor, is neuroprotective in mouse models of Huntington's disease. *J Huntingtons Dis* 5:347–355.

34. Hockly E, et al. (2003) Suberoylanilide hydroxamic acid, a histone deacetylase inhibitor, ameliorates motor deficits in a mouse model of Huntington's disease. *Proc Natl Acad Sci USA* 100:2041–2046.

35. Mielcarek M, et al. (2011) SAHA decreases HDAC 2 and 4 levels in vivo and improves molecular phenotypes in the R6/2 mouse model of Huntington's disease. *PLoS One* 6:e27746.

36. Hogarth P, Lovrecic L, Krainc D (2007) Sodium phenylbutyrate in Huntington's disease: A dose-finding study. *Mov Disord* 22:1962–1964.

37. Marques JM, Olsson IA, Ogren SO, Dahlborn K (2008) Evaluation of exploration and risk assessment in pre-weaning mice using the novel cage test. *Physiol Behav* 93:139–147.

38. Zabel C, et al. (2009) A large number of protein expression changes occur early in life and precede phenotype onset in a mouse model for Huntington disease. *Mol Cell Proteomics* 8:720–734.

39. Metzler M, et al. (2010) Phosphorylation of huntingtin at Ser421 in YAC128 neurons is associated with protection of YAC128 neurons from NMDA-mediated excitotoxicity and is modulated by PP1 and PP2A. *J Neurosci* 30:14318–14329.

40. Lewandowski NM, et al. (2013) Regional vulnerability in Huntington's disease: fMRI-guided molecular analysis in patients and a mouse model of disease. *Neurobiol Dis* 52:84–93.

41. Barresi M, et al. (2012) Evaluation of olfactory dysfunction in neurodegenerative diseases. *J Neurol Sci* 323:16–24.

42. Winner B, Kohl Z, Gage FH (2011) Neurodegenerative disease and adult neurogenesis. *Eur J Neurosci* 33:1139–1151.

43. Young SZ, Taylor MM, Bordey A (2011) Neurotransmitters couple brain activity to subventricular zone neurogenesis. *Eur J Neurosci* 33:1123–1132.

44. Schrödl F, et al. (2014) Rat choroidal pericytes as a target of the autonomic nervous system. *Cell Tissue Res* 356:1–8.

45. Brown JP, et al. (2003) Transient expression of doublecortin during adult neurogenesis. *J Comp Neurol* 467:1–10.

46. Blockx I, et al. (2012) Microstructural changes observed with DKI in a transgenic Huntington rat model: Evidence for abnormal neurodevelopment. *Neuroimage* 59:957–967.

47. Pipalia NH, et al. (2011) Histone deacetylase inhibitor treatment dramatically reduces cholesterol accumulation in Niemann-Pick type C1 mutant human fibroblasts. *Proc Natl Acad Sci USA* 108:5620–5625.

48. Siebzehnrubl FA, et al. (2007) Histone deacetylase inhibitors increase neuronal differentiation in adult forebrain precursor cells. *Exp Brain Res* 176:672–678.

49. Crittenden JR, et al. (2010) CalDAG-GEFI down-regulation in the striatum as a neuroprotective change in Huntington's disease. *Hum Mol Genet* 19:1756–1765.

50. Semple BD, Blomgren K, Gimlin K, Ferriero DM, Noble-Haeusslein LJ (2013) Brain development in rodents and humans: Identifying benchmarks of maturation and vulnerability to injury across species. *Prog Neurobiol* 106-107:1–16.

51. Hult Lundh S, Nilsson N, Soylu R, Kirik D, Petersén Å (2013) Hypothalamic expression of mutant huntingtin contributes to the development of depressive-like behavior in the BAC transgenic mouse model of Huntington's disease. *Hum Mol Genet* 22:3485–3497.

52. L'Episcopo F, et al. (2016) GSK-3β-induced Tau pathology drives hippocampal neuronal cell death in Huntington's disease: Involvement of astrocyte-neuron interactions. *Cell Death Dis* 7:e2206.

53. Brusilow WS (2006) Is Huntington's a glutamine storage disease? *Neuroscientist* 12:300–304.

54. Lee JK, et al. (2012) Measures of growth in children at risk for Huntington disease. *Neurology* 79:668–674.

55. Weeks RA, Piccini P, Harding AE, Brooks DJ (1996) Striatal D1 and D2 dopamine receptor loss in asymptomatic mutation carriers of Huntington's disease. *Ann Neurol* 40:49–54.

56. Ginovart N, et al. (1997) PET study of the pre- and post-synaptic dopaminergic markers for the neurodegenerative process in Huntington's disease. *Brain* 120:503–514.

57. Filloux F, et al. (1990) Nigral dopamine type-1 receptors are reduced in Huntington's disease: A postmortem autoradiographic study using [3H]SCH 23390 and correlation with [3H]forskolin binding. *Exp Neurol* 110:219–227.

58. Richfield EK, O'Brien CF, Eskin T, Shoulson I (1991) Heterogeneous dopamine receptor changes in early and late Huntington's disease. *Neurosci Lett* 132:121–126.

59. Glass M, Dragunow M, Faull RL (2000) The pattern of neurodegeneration in Huntington's disease: A comparative study of cannabinoid, dopamine, adenosine and GABA(A) receptor alterations in the human basal ganglia in Huntington's disease. *Neuroscience* 97:505–519.

60. Sedvall G, et al. (1994) Dopamine D1 receptor number–A sensitive PET marker for early brain degeneration in Huntington's disease. *Eur Arch Psychiatry Clin Neurosci* 243:249–255.

61. Turjanski N, Weeks R, Dolan R, Harding AE, Brooks DJ (1995) Striatal D1 and D2 receptor binding in patients with Huntington's disease and other choreas. A PET study. *Brain* 118:689–696.

62. Bibb JA, et al. (2000) Severe deficiencies in dopamine signaling in presymptomatic Huntington's disease mice. *Proc Natl Acad Sci USA* 97:6809–6814.

63. Greenamyre JT, et al. (1985) Alterations in L-glutamate binding in Alzheimer's and Huntington's diseases. *Science* 227:1496–1499.

64. Young AB, et al. (1988) NMDA receptor losses in putamen from patients with Huntington's disease. *Science* 241:981–983.

65. Albin RL, et al. (1990) Abnormalities of striatal projection neurons and N-methyl-D-aspartate receptors in presymptomatic Huntington's disease. *N Engl J Med* 322:1293–1298.

66. Milnerwood AJ, et al. (2010) Early increase in extrasynaptic NMDA receptor signaling and expression contributes to phenotype onset in Huntington's disease mice. *Neuron* 65:178–190.

67. Cowan CM, et al. (2008) Polyglutamine-modulated striatal calpain activity in YAC transgenic Huntington disease mouse model: Impact on NMDA receptor function and toxicity. *J Neurosci* 28:12725–12735.

68. Dunah AW, Standaert DG (2001) Dopamine D1 receptor-dependent trafficking of striatal NMDA glutamate receptors to the postsynaptic membrane. *J Neurosci* 21:5546–5558.

69. André VM, Cepeda C, Levine MS (2010) Dopamine and glutamate in Huntington's disease: A balancing act. *CNS Neurosci Ther* 16:163–178.

70. Lee FJ, Liu F (2004) Direct interactions between NMDA and D1 receptors: A tale of tails. *Biochem Soc Trans* 32:1032–1036.

71. Gheusi G, Ortega-Perez I, Murray K, Lledo PM (2009) A niche for adult neurogenesis in social behavior. *Behav Brain Res* 200:315–322.

72. Nguyen GD, Gokhan S, Molero AE, Mehler MF (2013) Selective roles of normal and mutant huntingtin in neural induction and early neurogenesis. *PLoS One* 8:e64368.

73. Walton NM, et al. (2006) Microglia instruct subventricular zone neurogenesis. *Glia* 54:815–825.

74. Gil JM, Leist M, Popovic N, Brundin P, Petersén A (2004) Asialoerythropoietin is not effective in the R6/2 line of Huntington's disease mice. *BMC Neurosci* 5:17.

75. Simpson JM, et al. (2011) Altered adult hippocampal neurogenesis in the YAC128 transgenic mouse model of Huntington disease. *Neurobiol Dis* 41:249–260.

76. Kohl Z, et al. (2010) Impaired adult olfactory bulb neurogenesis in the R6/2 mouse model of Huntington's disease. *BMC Neurosci* 11:114.

77. Fedele V, Roybon L, Nordström U, Li JY, Brundin P (2011) Neurogenesis in the R6/2 mouse model of Huntington's disease is impaired at the level of NeuroD1. *Neuroscience* 173:76–81.

78. Kandasamy M, et al. (2015) Reduction in subventricular zone-derived olfactory bulb neurogenesis in a rat model of Huntington's disease is accompanied by striatal invasion of neuroblasts. *PLoS One* 10:e0116069.

79. Curtis MA, et al. (2003) Increased cell proliferation and neurogenesis in the adult human Huntington's disease brain. *Proc Natl Acad Sci USA* 100:9023–9027.

80. Kántor O, et al. (2006) Selective striatal neuron loss and alterations in behavior correlate with impaired striatal function in Huntington's disease transgenic rats. *Neurobiol Dis* 22:538–547.

81. Bode FJ, et al. (2008) Sex differences in a transgenic rat model of Huntington's disease: Decreased 17beta-estradiol levels correlate with reduced numbers of DARPP32+ neurons in males. *Hum Mol Genet* 17:2595–2609.

82. Cha JH (2007) Transcriptional signatures in Huntington's disease. *Prog Neurobiol* 83:228–248.

83. Nguyen HP, et al. (2008) Age-dependent gene expression profile and protein expression in a transgenic rat model of Huntington's disease. *Proteomics Clin Appl* 2:1638–1650.

84. Steffan JS, et al. (2001) Histone deacetylase inhibitors arrest polyglutamine-dependent neurodegeneration in Drosophila. *Nature* 413:739–743.

85. Ferrante RJ, et al. (2003) Histone deacetylase inhibition by sodium butyrate chemotherapy ameliorates the neurodegenerative phenotype in Huntington's disease mice. *J Neurosci* 23:9418–9427.

NEUROSCIENCE

86. Beckers T, et al. (2007) Distinct pharmacological properties of second generation HDAC inhibitors with the benzamide or hydroxamate head group. *Int J Cancer* 121: 1138–1148.

87. von Hörsten S, et al. (2003) Transgenic rat model of Huntington's disease. *Hum Mol Genet* 12:617–624.

88. Gray M, et al. (2008) Full-length human mutant huntingtin with a stable polyglutamine repeat can elicit progressive and selective neuropathogenesis in BACHD mice. *J Neurosci* 28:6182–6195.

89. Kilkenny C, Browne W, Cuthill IC, Emerson M, Altman DG (2010) Animal research: Reporting in vivo experiments: The ARRIVE guidelines. *Br J Pharmacol* 160: 1577–1579.

90. Urbach YK, Bode FJ, Nguyen HP, Riess O, von Hörsten S (2010) Neurobehavioral tests in rat models of degenerative brain diseases. *Methods Mol Biol* 597: 333–356.

91. Couillard-Despres S, et al. (2006) Targeted transgene expression in neuronal precursors: Watching young neurons in the old brain. *Eur J Neurosci* 24:1535–1545.